

# A D-Band SPDT Switch Utilizing Reverse-Saturated SiGe HBTs for Dicke-Radiometers

Barbaros Cetindogan\*, Berkutug Ustundag<sup>†</sup>, Esref Turkmen<sup>‡</sup>, Matthias Wietstruck\*, Mehmet Kaynak\*<sup>‡</sup>  
and Yasar Gurbuz<sup>‡</sup>

\*IHP, Im Technologiepark 25, 15236 Frankfurt (Oder), Germany

<sup>†</sup>University of California, San Diego, 9500 Gilman Drive, La Jolla, CA 92093, USA

<sup>‡</sup>Sabanci University, Orta Mahalle, Universite Cd. No:27, 34956 Istanbul, Turkey

Email: yasar@sabanciuniv.edu

**Abstract**—This paper presents a low insertion loss and high isolation D-band (110-170 GHz) single-pole double-throw (SPDT) switch utilizing reverse-saturated SiGe HBTs for Dicke-radiometers. The SPDT switch design is based on the quarter-wave shunt switch topology and implemented with further optimizations to improve the overall insertion loss and decrease the total chip size in a commercial 0.13- $\mu\text{m}$  SiGe BiCMOS technology. Measurement results of the implemented SPDT switch show a minimum insertion loss of 2.6 dB at 125 GHz and a maximum isolation of 30 dB at 151 GHz while the measured input and output return loss is greater than 10 dB across 110-170 GHz. Total power consumption of the SPDT switch is 5.3 mW while draining 5.6 mA from a 0.95 V DC supply. Overall chip size is only  $0.5 \times 0.32 = 0.16 \text{ mm}^2$ , excluding the RF and DC pads.

**Index Terms**—millimeter-wave integrated circuits, single-pole double-throw (SPDT) switch, SiGe BiCMOS, Radiometers

## I. INTRODUCTION

The rapid improvements in silicon-based technologies such as CMOS and SiGe BiCMOS as well as the increasing demand on the imaging systems in the recent years have pushed the advancements in the millimeter-wave and THz region monolithic integrated circuits (MMICs) and systems. Millimeter-wave radiometer systems, also called as millimeter-wave passive imagers, are systems which are capable of operating around low atmospheric attenuation windows such as 94, 140 and 220 GHz which can detect the thermal radiation emitted from the objects in low visibility conditions. However, achieving low noise equivalent temperature difference (NETD) values is still a challenging issue in these systems. The most important limiting factor for achieving low NETD values in radiometer systems arises from the  $1/f$  noise of active components in the system architectures. Thus, periodic calibration techniques such as Dicke-switching which shifts the output spectrum of the system to a switching frequency higher than the  $1/f$  noise corner of system are used commonly used in radiometer systems to improve the system NETD [1].

As stated above, when operated as a Dicke-switch, single-pole double-throw (SPDT) switches become a critical building block for the millimeter-wave passive imaging systems. Therefore, a careful optimization is required for the SPDT switches which will be implemented in a Dicke-radiometer system in order to provide an acceptable NETD improvement. A low insertion

loss of  $\sim 3$  dB and an isolation of  $\sim 20$  dB are the commonly desired features of such an SPDT switch. Since achieving high performance is the most critical parameter in most of the millimeter-wave systems, the SPDT switches implemented in these systems were also mostly implemented in III-V technologies [2]–[4]. But with the recent improvements in the silicon-based technologies, high performance millimeter-wave SPDT switch designs in CMOS [5]–[7] and SiGe BiCMOS technologies [8]–[10] have been reported in the literature which can compete with their III-V counterparts.

This paper focuses on the design of a D-band (110-170 GHz) SPDT switch utilizing reverse-saturated SiGe HBTs in order to achieve low insertion loss and high isolation for high performance, silicon-based Dicke-radiometer systems. Section II discusses about the circuit level descriptions and design of the implemented SPDT switch in detail. Measurement results of the SPDT switch are discussed in Section III and Section IV concludes the paper.

## II. CIRCUIT DESIGN

Detailed schematic of the implemented D-band SPDT switch design is presented in Fig. 1. The design is based on the quarter-wave shunt switch topology and implemented with further optimizations in order to achieve low insertion loss at the millimeter-wave frequencies. The use of HBT devices as series switches in millimeter-wave SPDT switch designs is limited since the overall insertion loss severely degrades due to the  $R_{on}$  resistance of the HBT devices. Therefore, HBT devices are only used as shunt switches in this design. This reduces the isolation between the output ports of the SPDT switch but keeps the insertion loss to a minimum.

In the quarter-wave shunt switch topology, when the  $V_{cont.}$  is at a low voltage and  $V_{\overline{cont.}}$  is at a high voltage, Q1 device is turned “off” and Q2 device is turned “on”. While turned “off”, the Q1 device represents a high impedance for the RF power traveling towards the  $RF_{out}$  port at the upper branch of the T-junction. Insertion loss of an SPDT switch is defined as total loss of the RF power reaching towards the  $RF_{out}$  port. Typically, a shunt transmission line is also included in the output matching network in order to resonate the parasitic device capacitance,  $C_{off}$ , to improve the overall insertion loss at the frequency of operation. The shunt transmission line also

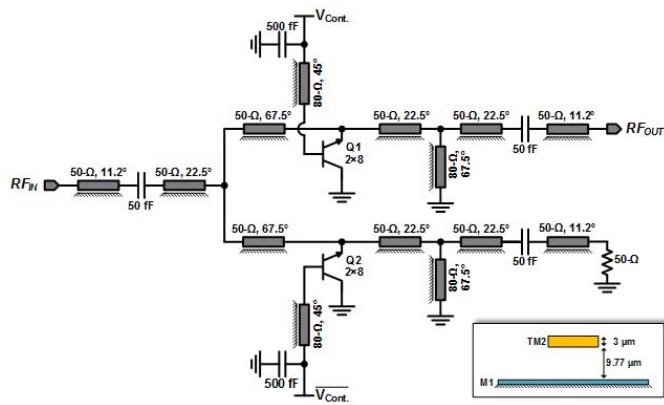


Fig. 1. Detailed schematic of the D-band SPDT switch with reverse-saturated HBTs

acts as a ground reference for the device. At the same time, the Q2 device is turned “on” and acts as a short circuit. The quarter-wave transmission line in the input matching network acts as an impedance inverter and transforms the short circuit into an open circuit. Thus, the RF power is prevented from traveling towards the lower branch of the T-junction. Isolation of an SPDT switch is defined as the total loss of RF power reaching towards the 50- $\Omega$  termination at the output of the lower branch of the T-junction.

There are two main factor associated with the overall insertion loss of a millimeter-wave SPDT switch using the quarter-wave shunt switch topology. The first and most dominant of these factors would be the parasitic effects associated with the HBTs when used as a shunt switch. When the device is turned “on”,  $R_{on}$  of the device must be as low as possible to ensure a high isolation value. Several shunt devices can be used to achieve a low  $R_{on}$  value. But using several shunt devices also results in a low  $R_{off}$  and high  $C_{off}$  values which degrades the insertion loss of the SPDT switch. The insertion loss if the SPDT switch is much more significant for the NETD value of the Dicke-radiometer systems than the isolation. Consequently, trade-offs need to be made when selecting the device sizes in order to improve the insertion loss of the SPDT switch. To further improve the insertion loss in this SPDT design, the shunt HBT devices are used in the reverse-saturation mode by connecting the emitter terminal of the device to the RF output and grounding the collector terminal. Using the shunt HBT switches in the reverse-saturation mode increases the  $R_{off}$  and decreases the  $C_{off}$  values with respect to the shunt HBT switches used in the forward-saturation mode [8], [9].

The other dominant factor associated with the insertion loss of the millimeter-wave SPDT switches is the passive components, transmission lines and tungsten vias in this case. It is not possible to avoid the loss due to the use of tungsten vias but the transmission lines in the design can be optimized such that the loss is minimized. The shunt HBT devices does not act as a perfect short when turned “on” due to the parasitic effects of the device. Thus, the quarter-wave transmission line, which contributes the most to the insertion loss amongst the

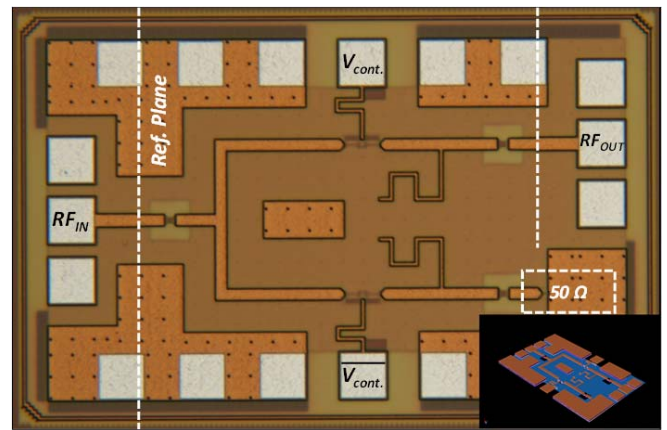


Fig. 2. Chip photo and the ADS Momentum EM-simulation environment of the D-band SPDT switch with reverse-saturated HBTs. Chip size is  $0.5 \times 0.32 = 0.16 \text{ mm}^2$ , excluding the RF and DC pads.

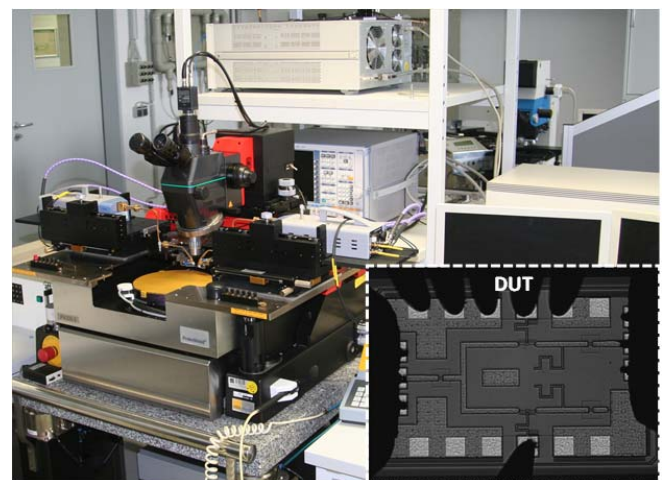


Fig. 3. Photo of the measurement setup and device under test.

matching networks in this topology, can be implemented with a shorter electrical length to improve the insertion loss. It should be noted that the overall chip size of the SPDT switch also decreases with this optimization.

As presented in the Fig. 1, input of the implemented SPDT switch consists of 50- $\Omega$  transmission lines with electrical lengths of  $22^\circ$  and  $67^\circ$  along with a 50 fF MIM capacitor which also facilitates the input matching and acts as a DC block. Two shunt HBTs with eight emitter stripes are implemented as shunt switches which corresponds to 5- $\Omega$   $R_{on}$  and 13 fF  $C_{off}$ . A 80- $\Omega$  shunt transmission line with electrical length of  $67^\circ$  is implemented at the output matching network in order to improve the insertion loss along with 50- $\Omega$ ,  $22^\circ$  transmission lines and a 50 fF MIM capacitor. Lastly, bias networks for the control voltages consists of of an 80- $\Omega$ ,  $45^\circ$  transmission line and a self-resonating 500 fF bypass capacitor. It should be noted that the electrical length of the transmission lines are defined at 140 GHz. Parasitic effects of the input and output RF pads have not been taken into account in the design since the SPDT will be used in a system without the pads.

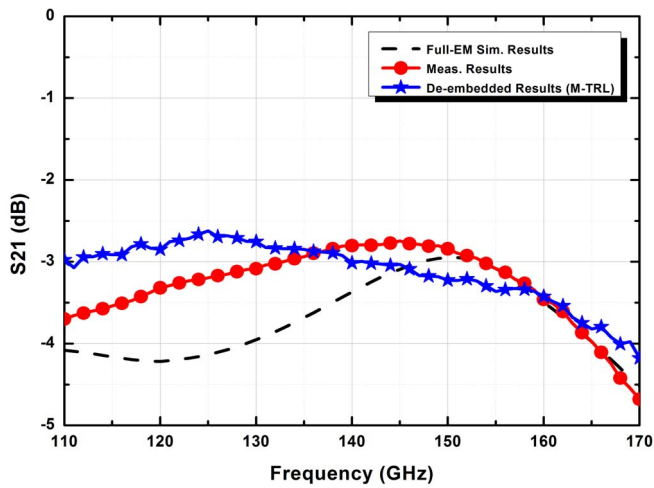


Fig. 4. Simulated and measured insertion loss of the D-band SPDT switch with reverse-saturated HBTs.

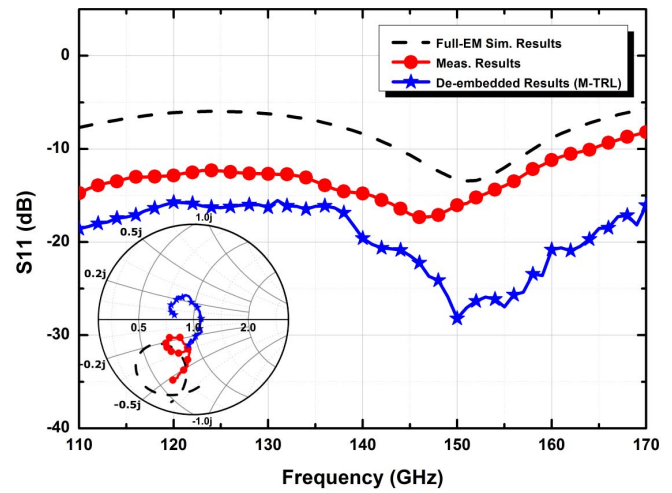


Fig. 6. Simulated and measured input return loss of the D-band SPDT switch with reverse-saturated HBTs.

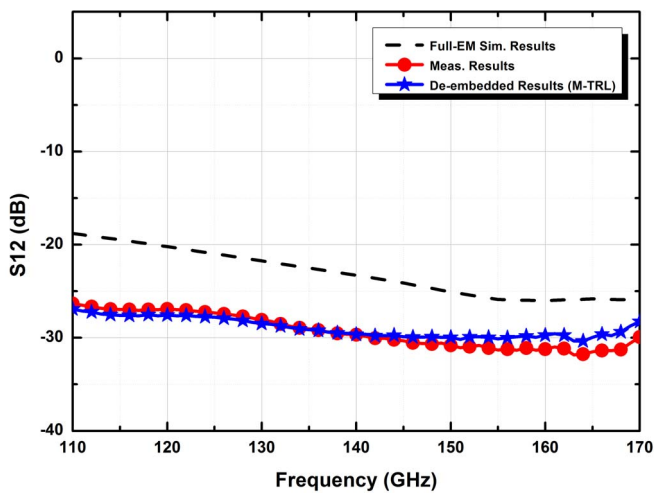


Fig. 5. Simulated and measured isolation of the D-band SPDT switch with reverse-saturated HBTs.

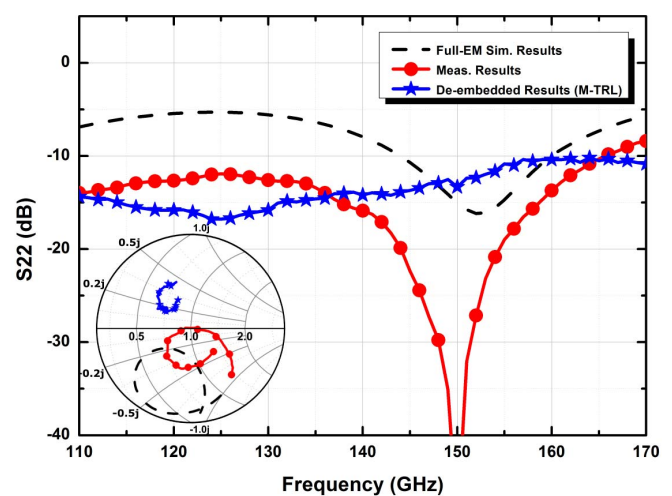


Fig. 7. Simulated and measured output return loss of the D-band SPDT switch with reverse-saturated HBTs.

### III. MEASUREMENT RESULTS

The D-band SPDT switch utilizing reverse-saturated HBTs was designed and fabricated in IHP SG13G2 SiGe BiCMOS technology in which the  $0.13\text{-}\mu\text{m}$  SiGe HBTs have  $f_T/f_{max}$  of 300/500 GHz. Input and output matching networks, along with the bias networks for the control voltages are designed as microstrip transmission lines by using the top and bottom metal layers available in the technology with the ADS Momentum EM-simulation software [11]. Chip photo and the EM-simulation environment of the SPDT design is presented in Fig. 2. Input and output RF pads were also included in the EM-simulation environment in order to validate the initial measurement results.  $V_{cont.}$  and  $V_{\overline{cont.}}$  applied to the base terminals of the shunt HBT devices in order to achieve the insertion loss and isolation cases are equal to 0 V and 0.95 V, respectively. Total power consumption of the SPDT switch is 5.3 mW. Overall chip size of the IC is only  $0.5 \times 0.32 = 0.16 \text{ mm}^2$ , excluding the RF and DC pads.

Two port S-parameter measurements of the D-band SPDT switch were performed on-wafer from 110 to 170 GHz while one of the outputs of the switch is terminated with an on-chip  $50\text{-}\Omega$ . The measurement setup consists of a Rhode & Schwarz ZVA24 VNA, ZC170 millimeter-wave converters and  $75\text{-}\mu\text{m}$  pitch sized Cascade Microtech Infinity D-band probes with WR-6 waveguide connections as shown in Fig. 3. The reference plane for the measurements was set to the probe tips by performing an LRRM calibration with using a Cascade ISS 138-356. The ISS was placed on an auxiliary alumina chuck on top of an RF-absorber. Later, a TRL calibration is also performed by using on-chip de-embedding structures to further set the reference plane on the die and de-embed the parasitic effects of the RF pads. Simulation and measurement results are presented in Fig. 4-7. Fig. 4 presents the simulation and measurement results for the insertion loss of the SPDT switch. The measurement results show that the minimum insertion loss of the SPDT switch is 2.6 dB at 125 GHz. The insertion

TABLE I  
PERFORMANCE SUMMARY AND COMPARISON TABLE

| Reference        | Technology                   | Topology  | Frequency (GHz) | Insertion Loss (dB) | Isolation (dB) | Power Consumption (mW) | Area (mm <sup>2</sup> ) |
|------------------|------------------------------|---|-----------------|---------------------|----------------|------------------------|-------------------------|
| [4]              | 50-nm<br>InAlGaAs HEMT       | Double-shunt                                    | 77-120          | 1.9                 | 35             | -                      | 0.75                    |
| [6]              | 32-nm<br>CMOS SOI            | Single Shunt                                    | 110-170         | 2.6                 | 22             | -                      | 0.21                    |
| [7]              | 65-nm<br>CMOS                | Magnetically Switchable<br>Artificial Resonator | 130-180         | 3.3                 | 23.7           | -                      | 0.0035*                 |
| [8]              | 90-nm<br>SiGe BiCMOS         | Reverse-saturated<br>Shunt HBTs                 | 77-110          | 1.4                 | 19.3           | 8                      | 0.14*                   |
| [9]              | 90-nm<br>SiGe BiCMOS         | Reverse-saturated<br>Shunt HBTs                 | 73-110          | 1.1                 | 22             | 5.9                    | 0.21*                   |
| [10]             | 0.13- $\mu$ m<br>SiGe BiCMOS | Double-shunt<br>Saturated HBTs                  | 110-170         | 2.6                 | 29             | 6                      | 0.36                    |
| <b>This work</b> | 0.13- $\mu$ m<br>SiGe BiCMOS | Reverse-saturated<br>Shunt HBTs                 | 110-170         | 2.6                 | 30             | 5.3                    | 0.16*                   |

\* Excluding the pads

loss remains above 3 dB between 110-145 GHz and above 4 dB between 110-168 GHz. As presented in Fig. 5, measured isolation is greater than 26 dB between 110-170 GHz with a maximum isolation of 30 dB at 151 GHz. Input and output return losses of the switch are displayed in Fig. 6 and Fig. 7, respectively. Both of the input and output return losses are better than 10 dB between 110-170 GHz.

Table I presents the performance summary of the D-band SPDT switch utilizing reverse-saturated HBTs and comparison of this work with other state-of-the-art millimeter-wave SPDT switches. The implemented SPDT switch design presented in this work also shows state-of-the-art performance among other reported works in the literature using CMOS and SiGe BiCMOS technologies along with the designs implemented in III-V technologies in the D-band frequency range.

#### IV. CONCLUSION

This paper has presented an investigation of the utilization of reverse-saturated shunt SiGe HBTs in D-band SPDT switches in order to achieve low insertion loss and high isolation for Dicke-radiometers. Measurement results of the SPDT switch implemented in a 0.13- $\mu$ m SiGe BiCMOS technology show a minimum insertion loss of 2.6 dB and maximum isolation of 30 dB while the input and output return loss is greater than 10 dB across the D-band frequency range. These results suggest a state-of-the-art performance when compared to the other works implemented with III-V, CMOS and SiGe BiCMOS technologies and proves that this topology is suitable to be implemented in high performance silicon-based millimeter-wave passive imaging systems.

#### ACKNOWLEDGMENT

This work is supported by the Scientific and Technological Research Council of Turkey under the grant 115E101.

#### REFERENCES

- [1] R. H. Dicke, "The Measurement of Thermal Radiation at Microwave Frequencies," *Review of Scientific Instruments*, vol. 17, no. 7, pp. 268–275, 1946.
- [2] J. Putnam, M. Fukuda, P. Staecker, and Y.-H. Yun, "A 94 GHz Monolithic Switch with a Vertical PIN Diode Structure," in *Proceedings of 1994 IEEE GaAs IC Symposium*, Oct 1994, pp. 333–336.
- [3] F. Steinhagen, H. Massler, W. H. Haydl, A. Hulsmann, and K. Kohler, "Coplanar W-Band SPDT and SPTT Resonated PIN Diode Switches," in *1999 29th European Microwave Conference*, vol. 2, Oct 1999, pp. 53–56.
- [4] I. Kallfass, S. Diebold, H. Massler, S. Koch, M. Seelmann-Eggebert, and A. Leuther, "Multiple-Throw Millimeter-Wave FET Switches for Frequencies from 60 up to 120 GHz," in *2008 European Microwave Integrated Circuit Conference*, Oct 2008, pp. 426–429.
- [5] M. Uzunkol and G. M. Rebeiz, "140-220 GHz SPST and SPDT Switches in 45 nm CMOS SOI," *IEEE Microwave and Wireless Components Letters*, vol. 22, no. 8, pp. 412–414, Aug 2012.
- [6] W. T. Khan, A. C. Ulusoy, R. Schmid, T. Chi, J. D. Cressler, H. Wang, and J. Papapolymerou, "A D-band (110 to 170 GHz) SPDT switch in 32 nm CMOS SOI," in *2015 IEEE MTT-S International Microwave Symposium*, May 2015, pp. 1–3.
- [7] F. Meng, K. Ma, and K. S. Yeo, "A 130-to-180 GHz 0.0035mm<sup>2</sup> SPDT Switch with 3.3dB Loss and 23.7dB Isolation in 65nm Bulk CMOS," in *2015 IEEE International Solid-State Circuits Conference - (ISSCC) Digest of Technical Papers*, Feb 2015, pp. 1–3.
- [8] R. L. Schmid, A. C. Ulusoy, P. Song, and J. D. Cressler, "A 94 GHz, 1.4 dB Insertion Loss Single-Pole Double-Throw Switch Using Reverse-Saturated SiGe HBTs," *IEEE Microwave and Wireless Components Letters*, vol. 24, no. 1, pp. 56–58, Jan 2014.
- [9] R. L. Schmid, P. Song, C. T. Coen, A. C. Ulusoy, and J. D. Cressler, "On the Analysis and Design of Low-Loss Single-Pole Double-Throw W-Band Switches Utilizing Saturated SiGe HBTs," *IEEE Transactions on Microwave Theory and Techniques*, vol. 62, no. 11, pp. 2755–2767, Nov 2014.
- [10] A. C. Ulusoy, P. Song, R. L. Schmid, W. T. Khan, M. Kaynak, B. Tillack, J. Papapolymerou, and J. D. Cressler, "A Low-Loss and High Isolation D-Band SPDT Switch Utilizing Deep-Saturated SiGe HBTs," *IEEE Microwave and Wireless Components Letters*, vol. 24, no. 6, pp. 400–402, June 2014.
- [11] Keysight Advanced Design System (ADS) [computer software].